

Multi-Trace Müller Boundary Integral Equation for Electromagnetic Scattering by Composite Objects

Van Chien Le, *Member, IEEE*, and Kristof Cools, *Member, IEEE*

arXiv:2601.13823v1 [math.NA] 20 Jan 2026

Abstract—This paper introduces a boundary integral equation for time-harmonic electromagnetic scattering by composite dielectric objects. The formulation extends the classical Müller equation to composite structures through the global multi-trace method. The key ingredient enabling this extension is the use of the Stratton–Chu representation in complementary region, also known as the extinction property, which augments the off-diagonal blocks of the interior representation operator. The resulting block system is composed entirely of second-kind operators. A Petrov–Galerkin (mixed) discretization using Rao–Wilton–Glisson trial functions and Buffa–Christiansen test functions is employed, yielding linear systems that remain well conditioned on dense meshes and at low frequencies without the need for additional stabilization. This reduces computational costs associated with matrix–vector multiplications and iterative solving. Numerical experiments demonstrate the accuracy of the method in computing field traces and derived quantities.

Index Terms—Müller boundary integral equation, global multi-trace formulation, composite objects, well-conditioning

I. INTRODUCTION

THE accurate modelling of composite electromagnetic systems is essential for the analysis and design of modern devices in antennas, propagation, microelectronics, and photonics. However, computing electromagnetic fields in the presence of heterogeneous materials and geometrically complex, multi-scale structures remains challenging. Among several numerical methods, boundary integral equation (BIE) formulations have emerged as a powerful and widely used approach. Their main advantage lies in the reduction of problem dimensionality, since only the interfaces of the domain require discretization, leading to a significant decrease in the number of unknowns compared to volumetric-based methods. Moreover, BIEs inherently satisfy the radiation condition, making them particularly effective for open-region scattering and radiation problems.

BIE formulations for composite electromagnetic problems differ primarily in how they enforce transmission conditions at interfaces between adjacent materials. Many approaches have been introduced over the years, most of them can be classified into the single-trace, local multi-trace, and global multi-trace formulations. In single-trace formulations, a single pair of

Manuscript received April 19, 2005; revised August 26, 2008; accepted 19 May 2014. Date of publication 12 June 2014; date of current version 9 July 2014. This work was supported by European Research Council (ERC) under European Union’s Horizon 2020 Research and Innovation Program under Grant 101001847. (Corresponding author: Van Chien Le.)

Van Chien Le and Kristof Cools are with IDLab, Department of Information Technology at Ghent University – imec, 9000 Ghent, Belgium (e-mail: vanchien.le@ugent.be, kristof.cools@ugent.be).

Color versions of one or more figures in this article are available at <https://doi.org/>

Digital Object Identifier

unknowns representing the tangential traces of the electric and magnetic fields is sought on each interface, thereby enforcing field continuity in a direct manner. In contrast, multi-trace methods introduce two independent pairs of traces on each interface, one for each neighbouring subdomain. Local multi-trace formulations combine the self-representing property of the tangential traces in each domain with the continuity conditions, resulting in a uniquely solvable system for the traces. Global multi-trace formulations, on the other hand, impose these conditions weakly by introducing a conceptual gap between adjacent regions. These distinctions lead to formulations defined on different trace spaces, and the differences become particularly pronounced in the presence of complex junctions where three or more regions meet.

Over the past decades, considerable efforts have been devoted to developing efficient and robust BIE solvers for composite electromagnetic scattering problems. First-kind formulations, despite their ill-conditioning, remain widely used due to their high accuracy and natural extension to composite structures. Single-trace extensions of the classical Poggio–Miller–Chang–Harrington–Wu–Tsai (PMCHWT) equation have been investigated in [1], [2], although stabilizing these formulations on dense meshes remains a significant challenge, especially in the presence of junctions. A quasi-local Calderón preconditioner recently proposed in [3] partially mitigates this difficulty and achieves nearly mesh-independent Krylov convergence. Local multi-trace methods have also been examined in [4]–[6], but their efficiency depends strongly on the discretization and on how the transmission conditions are enforced. The global multi-trace PMCHWT formulation was independently explored in [7]–[9], where its well-posedness was established, and low-frequency stabilization and dense-mesh preconditioning strategies were introduced. This framework was later extended to structures involving screens and perfect electric conductors (PECs) in [10]. Nevertheless, a first-kind formulation that is simultaneously efficient, accurate, and robust for general composite configurations across broad frequency ranges is still lacking.

In contrast to first-kind BIEs, second-kind formulations, such as the magnetic field integral equation for PECs and the Müller equation for dielectrics [11], are intrinsically well-conditioned, leading to fast convergence of iterative solvers on a wide range of frequencies and mesh densities. They were historically perceived as less accurate than their first-kind counterparts [12]–[14]. However, the development of dual basis functions, such as the Buffa–Christiansen (BC) [15] and Chen–Wilton (CW) [16] functions, has enabled conforming mixed discretizations that preserve the favorable conditioning of second-kind equations while achieving accuracy compa-

able to that of first-kind formulations and improving low-frequency behavior [17]–[22]. Unfortunately, these advantages do not readily extend to composite objects involving junctions. It remained unclear how to cancel the hyper-singularities of all participating single-layer operators in multi-component settings [23], [24], which is the key mechanism underlying the superior conditioning of the Müller equation. The single-trace Müller formulation introduced in [25] represents a significant step forward by enabling this singularity cancellation through the incorporation of the multi-potential representation. Its discontinuous Galerkin discretization using piecewise-constant basis functions yields rapidly convergent systems. Nevertheless, the non-conforming nature of this scheme introduces low-frequency instabilities and degrades the accuracy of secondary quantities, such as far-field evaluations. More broadly, this issue reflects a fundamental limitation of single-trace formulations for composite structures: no discrete dual of single-trace energy spaces exists on interfaces that contain junctions. As a result, constructing effective Calderón preconditioners for first-kind BIEs and conforming mixed discretizations of second-kind equations within the single-trace framework becomes extremely challenging.

In this paper, we introduce a global multi-trace Müller formulation for electromagnetic scattering by arbitrary composite dielectric objects. In contrast to the single-trace approach in [25], the proposed formulation is derived through the use of the Stratton–Chu representation in the complementary region, i.e., exploiting the extinction property. The off-diagonal blocks of the interior boundary representation operator are augmented with the tangential traces, taken on the boundary of the row subdomain, of the potential operators associated with the column subdomain. This augmentation enables a consistent linear combination of the exterior and interior representation formulas that eliminates the hyper-singularities in all block-matrix entries, resulting in a system composed entirely of second-kind operators. A key advantage of the proposed formulation is that it admits a conforming mixed discretization, based on trial and dual basis functions defined on the full boundary of each subdomain. This provides, for the first time, a second-kind multi-trace formulation for composite dielectric scattering that is both conforming and applicable in the presence of junctions, thereby overcoming the instabilities inherent in existing first-kind or non-conforming second-kind schemes. Numerical experiments demonstrate that the new formulation achieves accurate field traces and derived quantities, while exhibiting significantly improved conditioning at low frequencies and on dense meshes. Moreover, despite the introduction of additional boundary integral operators (BIOS) and dual test functions, the overall computational cost remains competitive with that of first-kind formulations, including Calderón-preconditioned (CP) variants, when the number of scattering components is moderate.

An important motivation for developing the global multi-trace Müller equation lies in its potential extension to time-domain (TD) problems. In this regime, PMCHWT formulations are known to suffer from late-time instabilities [26]. Although stabilization strategies for TD-PMCHWT equations have been proposed, they typically lead to substantially more

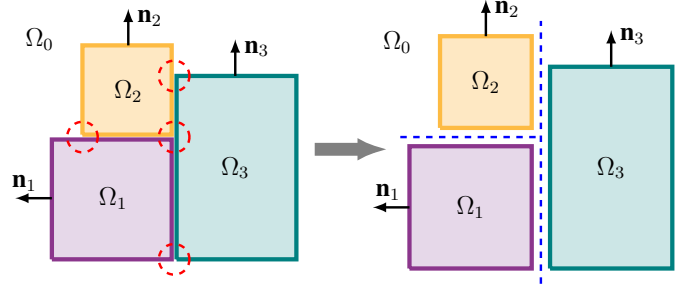


Fig. 1. *Left*: A composite object consisting of several components $\Omega_k, k = 1, 2, \dots, N$, immersed in the background Ω_0 . This configuration usually gives rise to junctions that are curves where three or more regions meet (dashed red circles). *Right*: Illustration of the global multi-trace approach, in which a conceptual gap filled by the background medium is inserted between adjacent components (dashed blue lines).

complex systems [27]. By contrast, the uniformly second-kind structure of the present formulation suggests improved stability in the time domain. A systematic investigation of the global multi-trace TD-Müller formulation is therefore a promising direction for future work.

The rest of this paper is structured as follows. The next section introduces the notation and derives the global multi-trace Müller formulation. Section III presents a conforming mixed discretization and analyzes its computational cost. A comprehensive set of numerical examples is provided in Section IV to validate the accuracy, robustness, and computational efficiency of the proposed method. Finally, concluding remarks are outlined in Section V.

II. FORMULATION

A. Problem Setting and Notations

We consider an electromagnetic scatterer composed of N bounded Lipschitz components Ω_k , with boundary $\Gamma_k := \partial\Omega_k$ and outward unit normal vector $\mathbf{n}_k, k = 1, 2, \dots, N$. The background region is denoted by $\Omega_0 := \mathbb{R}^3 \setminus \bigcup_{k=1}^N \overline{\Omega_k}$ (see Fig. 1, *left*). Each region $\Omega_i, i = 0, 1, \dots, N$, is filled by a homogeneous, isotropic, dielectric material characterized by the coefficient matrix $\beta_i = \text{diag}(\epsilon_i, \mu_i)$, where ϵ_i and μ_i are the permittivity and permeability, respectively.

For clarity, throughout the paper, the index $i = 0, 1, \dots, N$ is used for $N + 1$ partitions of \mathbb{R}^3 (called regions), whereas the indices $j, k = 1, 2, \dots, N$ refer to the N components of the scatterer (also called subdomains).

The scatterer is illuminated by time-harmonic incident electric and magnetic fields $(\mathbf{e}^{inc}, \mathbf{h}^{inc})$ with angular frequency ω . The representation theorem states that any electromagnetic fields (\mathbf{e}, \mathbf{h}) satisfying Maxwell's equations in a subdomain $\Omega_k, k = 1, 2, \dots, N$, can be represented by equivalent surface currents on its boundary Γ_k . More precisely, the Stratton–Chu representation formula associated with the subdomain Ω_k reads [28]

$$\begin{aligned} & \begin{pmatrix} \mathcal{K}_k^{(k)} & -\eta_k \mathcal{T}_k^{(k)} \\ \eta_k^{-1} \mathcal{T}_k^{(k)} & \mathcal{K}_k^{(k)} \end{pmatrix} \begin{pmatrix} \mathbf{e} \times \mathbf{n}_k \\ \mathbf{n}_k \times \mathbf{h} \end{pmatrix} \\ &= \begin{cases} (\mathbf{e}, -\mathbf{h})^\top & \text{if } \mathbf{x} \in \Omega_k \\ (\mathbf{0}, \mathbf{0})^\top & \text{if } \mathbf{x} \in \mathbb{R}^3 \setminus \overline{\Omega_k}, \end{cases} \end{aligned} \quad (1)$$

where the single- and double-layer potentials are defined by

$$\begin{aligned}\mathcal{T}_k^{(i)}(\mathbf{m})(\mathbf{x}) &= -\iota\kappa_i \int_{\Gamma_k} \frac{e^{-\iota\kappa_i|\mathbf{x}-\mathbf{y}|}}{4\pi|\mathbf{x}-\mathbf{y}|} \mathbf{m}(\mathbf{y}) \, ds_{\mathbf{y}} \\ &\quad + \frac{1}{\iota\kappa_i} \mathbf{grad} \int_{\Gamma_k} \frac{e^{-\iota\kappa_i|\mathbf{x}-\mathbf{y}|}}{4\pi|\mathbf{x}-\mathbf{y}|} \operatorname{div}_{\Gamma} \mathbf{m}(\mathbf{y}) \, ds_{\mathbf{y}}, \\ \mathcal{K}_k^{(i)}(\mathbf{m})(\mathbf{x}) &= \mathbf{curl} \int_{\Gamma_k} \frac{e^{-\iota\kappa_i|\mathbf{x}-\mathbf{y}|}}{4\pi|\mathbf{x}-\mathbf{y}|} \mathbf{m}(\mathbf{y}) \, ds_{\mathbf{y}},\end{aligned}$$

with $i = 0, 1, \dots, N$, and $\mathbf{y} \in \Gamma_k$, $\mathbf{x} \notin \Gamma_k$, $k = 1, 2, \dots, N$. Here, ι denotes the imaginary unit, $\kappa_i = \omega\sqrt{\mu_i\epsilon_i}$ is the wavenumber, and $\eta_i = \sqrt{\mu_i/\epsilon_i}$ is the impedance coefficient. In the background region Ω_0 , the representation formula (1) holds for the scattered electromagnetic fields, which satisfy Maxwell's equations together with the radiation condition. The formula (1) is also known as the extinction property, meaning that the potential operators associated with one domain reconstruct its fields in the interior but vanish when evaluated outside that domain. The Stratton–Chu representation plays a central role in the construction of BIE formulations for electromagnetic scattering problems.

Taking the tangential traces of the potential operators yields the single-layer and double-layer BIOs

$$T_{jk}^{(i)} := \mathbf{n}_j \times \mathcal{T}_k^{(i)}, \quad K_{jk}^{(i)} := \mathbf{n}_j \times p.v. \mathcal{K}_k^{(i)},$$

where $p.v.$ stands for the Cauchy principal value, with $i = 0, 1, \dots, N$, and $j, k = 1, 2, \dots, N$. The following matrix BIO, which has a similar structure to the matrix potential operator in (1), is essential for assembling block matrices in the next sections:

$$A_{jk}^{(i)} := \begin{pmatrix} K_{jk}^{(i)} & -\eta_i T_{jk}^{(i)} \\ \eta_i^{-1} T_{jk}^{(i)} & K_{jk}^{(i)} \end{pmatrix}.$$

The operator $A_{jk}^{(i)}$ maps a pair of tangential traces on Γ_k to a pair of tangential traces on Γ_j and comprises BIOs defined with respect to the material parameters (ϵ_i, μ_i) .

For the testing, we also introduce the following local pairing between two pairs $(\mathbf{p}, \mathbf{q})^T$ and $(\mathbf{j}, \mathbf{m})^T$ of tangential traces supported on the boundary Γ_k :

$$\left\langle \begin{pmatrix} \mathbf{p} \\ \mathbf{q} \end{pmatrix}, \begin{pmatrix} \mathbf{j} \\ \mathbf{m} \end{pmatrix} \right\rangle_{\times, k} = \int_{\Gamma_k} (\mathbf{n}_k \times \mathbf{p}) \cdot \mathbf{j} + (\mathbf{n}_k \times \mathbf{q}) \cdot \mathbf{m} \, ds. \quad (2)$$

B. Global Multi-Trace Method

The global multi-trace approach seeks the tangential traces of the electric and magnetic fields on the boundary of each component Ω_k , $k = 1, 2, \dots, N$. On exterior interfaces that are parts of the boundary of Ω_0 , each trace appears only once. In contrast, on interior interfaces shared by two adjacent components, the traces are duplicated, one for each side of the interface. This distinction can be interpreted in terms of the introduction of an infinitesimally thin gap, so that all N components are treated as floating within the background medium Ω_0 and every subdomain contributes its own set of traces to the global system (see Fig. 1, right) [9].

Let us denote $\mathbf{u} := (\mathbf{u}_1, \mathbf{u}_2, \dots, \mathbf{u}_N)^T$, where $\mathbf{u}_k = (\mathbf{e} \times \mathbf{n}_k, \mathbf{n}_k \times \mathbf{h})^T$ is the local Cauchy data representing the equivalent magnetic and electric surface current densities on

the boundary Γ_k . We assume that the incident fields originate from the background region Ω_0 and satisfy Maxwell's equations there. The exterior boundary representation formula is obtained by taking the tangential traces of the Stratton–Chu formula associated with Ω_0 , from the interior of Ω_0 to the boundary of each subdomain Ω_k , $k = 1, 2, \dots, N$. Since the normal vector on Γ_k is oriented outward from Ω_k , we get

$$C^{(ext)} \mathbf{u} = -\mathbf{u}^{inc}, \quad (3)$$

where the right-hand vector $\mathbf{u}^{inc} = (\mathbf{u}_1^{inc}, \mathbf{u}_2^{inc}, \dots, \mathbf{u}_N^{inc})^T$, with $\mathbf{u}_k^{inc} = (\mathbf{e}^{inc} \times \mathbf{n}_k, \mathbf{n}_k \times \mathbf{h}^{inc})^T$. The $N \times N$ block-matrix operator $C^{(ext)}$, which describes the interaction between sub-domains through the background medium, is defined block-wise by [10]

$$\left[C^{(ext)} \right]_{jk} = A_{jk}^{(0)} - \frac{1}{2} I, \quad j, k = 1, 2, \dots, N,$$

where I is a so-called geometric identity, as introduced in [10]. This means, in theory, the identity operator in the off-diagonal blocks is included only when Γ_j and Γ_k share a common interface. In practical boundary-element implementations, however, it is unnecessary to distinguish explicitly between overlapping and non-overlapping interfaces when deriving the formulation. The geometric support of the basis functions implicitly enforces this distinction: when the two boundaries are disjoint, the corresponding discretized operator simply reduces to a zero matrix.

The interior boundary representation formula is derived analogously by taking the tangential traces of the Stratton–Chu formula (1) associated with each Ω_k , $k = 1, 2, \dots, N$, from the interior of Ω_k to its boundary Γ_k , yielding

$$C^{(int)} \mathbf{u} = \mathbf{0}, \quad (4)$$

where the block-diagonal operator $C^{(int)}$ is defined by

$$\left[C^{(int)} \right]_{kk} = A_{kk}^{(k)} + \frac{1}{2} I, \quad k = 1, 2, \dots, N.$$

The exterior and interior representation formulas (3) and (4) alone do not provide a unique solution for the Cauchy data \mathbf{u} . They must be combined into a single formulation that enforces the transmission conditions appropriately. The most widely used approach is the global multi-trace (MT-) PMCHWT equation, obtained by summing the two representations [9]

$$P\mathbf{u} := \left(C^{(ext)} + C^{(int)} \right) \mathbf{u} = -\mathbf{u}^{inc}. \quad (5)$$

The blocks of the operator P are given by

$$[P]_{kk} = A_{kk}^{(0)} + A_{kk}^{(k)}, \quad [P]_{jk} = A_{jk}^{(0)} - \frac{1}{2} I \quad (j \neq k).$$

The MT-PMCHWT formulation (5) is a first-kind BIE. In the next section, we derive a second-kind global multi-trace formulation based on the Müller equation.

C. Multi-Trace Müller Formulation

In contrast to the PMCHWT equation, the Müller formulation is constructed as a weighted linear combination of the exterior and interior representation formulas, with the weights chosen in terms of the material coefficients, such

that the hyper-singularities of the single-layer operators cancel. Following this principle, we consider the formulation

$$Q\mathbf{u} := \left(BC^{(int)} - B_0 C^{(ext)} \right) \mathbf{u} = B_0 \mathbf{u}^{inc}, \quad (6)$$

where the coefficient matrices

$$B_0 = \text{diag}(\beta_0, \beta_0, \dots, \beta_0), \quad B = \text{diag}(\beta_1, \beta_2, \dots, \beta_N).$$

The operator Q can be determined block-wise by

$$\begin{aligned} [Q]_{kk} &= \frac{1}{2} (\beta_k + \beta_0) I + \beta_k A_{kk}^{(k)} - \beta_0 A_{kk}^{(0)}, \\ [Q]_{jk} &= \frac{1}{2} \beta_0 I - \beta_0 A_{jk}^{(0)} \quad (j \neq k). \end{aligned}$$

The diagonal blocks of Q contain no hyper-singular terms, and are therefore second-kind operators. In contrast, the off-diagonal blocks exhibit hyper-singularity, which can result in ill-conditioned linear systems when discretized on dense meshes and at low frequencies. This inconsistency has contributed to the long-standing perception that the singularity-cancellation mechanism underlying the Müller equation breaks down in composite configurations [23].

The authors of [25] resolved this issue by leveraging the so-called multi-potential representation formula, which exploits the inherent continuity of the single-trace solutions to regularize the system and obtain a fully consistent second-kind equation. That technique, however, is not applicable in our global multi-trace framework, as the background region is treated differently from the N subdomains of the scatterer. In particular, on exterior interfaces, we consider only one pair of trace unknowns instead of two, and therefore the multi-potential formula does not hold on those interfaces.

In this contribution, we rely on the Stratton–Chu representation formula to regularize the Müller formulation. More specifically, for each pair $j \neq k$, we augment the off-diagonal block jk of the interior representation formula with the tangential traces of the Stratton–Chu potentials associated with the subdomain Ω_k , evaluated from the exterior of Ω_k onto the boundary Γ_j . The modified interior representation operator is defined as

$$\begin{aligned} \left[\widehat{C}^{(int)} \right]_{kk} &= \left[C^{(int)} \right]_{kk} = A_{kk}^{(k)} + \frac{1}{2} I, \\ \left[\widehat{C}^{(int)} \right]_{jk} &= \beta_j^{-1} \beta_k \left(A_{jk}^{(k)} - \frac{1}{2} I \right) \quad (j \neq k). \end{aligned} \quad (7)$$

Due to the extinction property, the augmented operators vanish when acting on the corresponding field traces; that is, for all $j, k = 1, 2, \dots, N$ and $j \neq k$

$$\left[\widehat{C}^{(int)} \right]_{jk} \mathbf{u}_k = \mathbf{0}.$$

Thus, the modified interior representation formula reads

$$\widehat{C}^{(int)} \mathbf{u} = \mathbf{0}. \quad (8)$$

Combining (8) with the exterior representation formula (3) yields the global multi-trace (MT-) Müller formulation

$$M\mathbf{u} := \left(B\widehat{C}^{(int)} - B_0 C^{(ext)} \right) \mathbf{u} = B_0 \mathbf{u}^{inc}, \quad (9)$$

where the block entries of M are given by

$$\begin{aligned} [M]_{kk} &= \frac{1}{2} (\beta_k + \beta_0) I + \beta_k A_{kk}^{(k)} - \beta_0 A_{kk}^{(0)}, \\ [M]_{jk} &= \frac{1}{2} (\beta_k - \beta_0) I + \beta_k A_{jk}^{(k)} - \beta_0 A_{jk}^{(0)} \quad (j \neq k). \end{aligned}$$

The material ratio $\beta_j^{-1} \beta_k$ appearing in (7) guarantees a consistent scaling across all blocks, thereby preserving the hyper-singularity cancellation mechanism. Consequently, every block of the operator M exhibits second-kind structure.

In the case of a single homogeneous dielectric (i.e., $N = 1$), the formulation (9) reduces to the classical Müller equation. If a component Ω_k is filled with the background medium, then all off-diagonal entries in the k th column of the operator M vanish, while the diagonal block becomes $\beta_0 I$. When all components coincide with the background medium (i.e., $B = B_0$), the formulation (9) degenerates to the trivial identity

$$B_0 \mathbf{u} = B_0 \mathbf{u}^{inc}. \quad (10)$$

III. DISCRETIZATION

Let the boundary Γ_k of subdomain $\Omega_k, k = 1, 2, \dots, N$, be discretized by a triangulation $\Gamma_{h,k}$ with average mesh size h , consisting of $N_{e,k}$ edges. The global mesh is defined as the disjoint union $\Gamma_h := \bigcup_{k=1}^N \Gamma_{h,k}$, which contains a total of $N_e := \sum_{k=1}^N N_{e,k}$ edges. It is worth noting that Γ_h needs not form a conformal mesh of the geometric skeleton $\bigcup_{k=1}^N \Gamma_k$. This flexibility is an inherent advantage of the multi-trace framework and enables the proposed method to efficiently handle large, multi-scale electromagnetic problems. Finally, although the notation Γ_h resembles the notation used for the boundaries Γ_k , the subscript h denotes discrete quantities and should not be interpreted as an index.

A. Mixed Discretization

The MT-Müller equation (9) is discretized using a conforming Petrov–Galerkin (mixed) scheme, employing Rao–Wilton–Glisson (RWG) basis functions [29] for the trial space and BC functions for the test space. The multi-trace trial space is defined as the direct product

$$\mathbb{RT}(\Gamma_h) := \prod_{k=1}^N \mathbb{RT}(\Gamma_{h,k}),$$

where $\mathbb{RT}(\Gamma_{h,k}) := \mathbb{RT}(\Gamma_{h,k}) \times \mathbb{RT}(\Gamma_{h,k})$, and $\mathbb{RT}(\Gamma_{h,k})$ is the boundary element space spanned by the $N_{e,k}$ RWG functions defined on the mesh $\Gamma_{h,k}$ of Γ_k . Analogously, the test space is defined as

$$\mathbb{BC}(\Gamma_h) := \prod_{k=1}^N \mathbb{BC}(\Gamma_{h,k}),$$

where $\mathbb{BC}(\Gamma_{h,k}) := \mathbb{BC}(\Gamma_{h,k}) \times \mathbb{BC}(\Gamma_{h,k})$, with $\mathbb{BC}(\Gamma_{h,k})$ spanned by the BC basis functions on $\Gamma_{h,k}$. This space is a discrete subspace of the multi-trace energy space and is locally dual to the trial space, meaning that the components associated with each subdomain are mutually dual.

The trace unknown \mathbf{u} is approximated by its expansion in $\mathbb{RT}(\Gamma_h)$ and the corresponding coefficient vector is denoted

by $\mathbf{u} \in \mathbb{C}^{2N_e}$. The mixed discrete formulation of (9) is then given by

$$\mathbb{M}\mathbf{u} = \mathbf{u}^{inc}, \quad (11)$$

where \mathbb{M} is the matrix representation of the bilinear form $\langle \cdot, M \cdot \rangle_{\times}$ on $\mathbb{BC}(\Gamma_h) \times \mathbb{RT}(\Gamma_h)$ with respect to its standard basis, and \mathbf{u}^{inc} is the coefficient vector representing the linear functional $\langle \cdot, B_0 \mathbf{u}^{inc} \rangle_{\times}$ on $\mathbb{BC}(\Gamma_h)$. Here, the global pairing $\langle \cdot, \cdot \rangle_{\times}$ is defined by

$$\langle \mathbf{f}, \mathbf{g} \rangle_{\times} := \sum_{k=1}^N \langle \mathbf{f}_k, \mathbf{g}_k \rangle_{\times,k}.$$

B. Computational Cost Analysis

The mixed discretization (11) yields linear systems that remain well conditioned across a wide range of frequencies and mesh densities. Consequently, iterative Krylov solvers converge rapidly without requiring any additional stabilization, thereby avoiding the cost associated with extra matrix-vector evaluations. Numerical results consistently demonstrate this advantage: the MT-Müller formulation achieves significantly shorter solving times than both the MT-PMCHWT equation and its CP variants. Although CP MT-PMCHWT formulations often exhibit a mesh-independent iteration count, their per-iteration matrix-vector multiplication costs grow quickly with mesh refinement and scale up the total solving time. This advantage of the MT-Müller formulation becomes even more pronounced when multiple right-hand sides are involved.

Despite these benefits, the MT-Müller equation presents two noteworthy drawbacks. The first stems from the mixed discretization of second-kind BIEs. Constructing BC test functions necessitates a barycentric refinement of the surface mesh, which increases the assembling time of the MT-Müller operator by roughly a factor of six compared with testing on the original mesh. It is worth noting, however, that efficient Calderón preconditioners for the PMCHWT formulation also rely on BC or CW functions and incur an even larger assembling cost, about 36 times that of the non-refined discretization. Refinement-free Calderón strategies [30] or OSRC preconditioners [31] can mitigate this burden, but they require non-trivial matrix manipulations or exhibit inconsistent performance across different frequency ranges.

The second drawback concerns the increased number of BIOs in the MT-Müller formulation. In the MT-PMCHWT equation (5), each diagonal block contains two single-layer and two double-layer operators, while each off-diagonal block consists of only one identity operator, one single-layer operator, and one double-layer operator (counting only unique operators due to symmetry). In contrast, every block of the MT-Müller operator in (9) includes one identity, two single-layer, and two double-layer operators. Although identity operators are local and can be assembled efficiently into sparse matrices, the additional non-local operators substantially increase the assembling time, especially for configurations with many scattering components.

In summary, the MT-Müller formulation offers superior solving times but higher assembling costs. For moderate numbers of sources and scattering components, its overall

computational cost is broadly comparable to that of the CP MT-PMCHWT equation. When the number of excitations increases, the MT-Müller equation becomes more efficient. Conversely, for large numbers of subdomains, the CP MT-PMCHWT approach is more favorable. The latter situation is typically not a limitation in practice, as hybrid finite-element-boundary-element coupling strategies generally outperform both formulations in such scenarios and thus constitute the preferred approach.

Finally, for a fixed number of components, the MT-Müller and MT-PMCHWT formulations exhibit similar asymptotic complexities when accelerated with hierarchical compression schemes such as Adaptive Cross Approximation (ACA) [32], [33], H-matrix method [34], or Fast Multipole Methods (FMMs) [35], [36].

IV. NUMERICAL RESULTS

In this section, we present numerical experiments that validate the accuracy, stability, and computational efficiency of the proposed MT-Müller formulation. The following three geometries with distinct configurations and material contrasts are considered (see Fig. 2):

- (a) A sphere of radius 1m, partitioned into two components: one occupying three quadrants and the other occupying the remaining quadrant. Both components are filled with the same material characterized by $(\epsilon, \mu) = (3\epsilon_0, \mu_0)$.
- (b) A dual-torus geometry formed by the intersection of two square-section tori of dimensions 1m \times 1m \times 0.25m and 0.75m \times 0.25m \times 0.75m, such that one cavity is completely occluded. The two subdomains are filled with materials $(\epsilon_1, \mu_1) = (2\epsilon_0, \mu_0)$ and $(\epsilon_2, \mu_2) = (4\epsilon_0, \mu_0)$.
- (c) A vertical stack (along the z -axis) of N cubes of side length 1m. The k th cube (counted from bottom to top) is filled with material $(\epsilon_k, \mu_k) = ((k+1)\epsilon_0, \mu_0)$.

Throughout this section, the background medium is free space, and the incident fields are the plane wave

$$\begin{aligned} \mathbf{e}^{inc}(\mathbf{x}) &= \hat{\mathbf{x}} \exp(-i\kappa_0 \hat{\mathbf{z}} \cdot \mathbf{x}), \\ \mathbf{h}^{inc}(\mathbf{x}) &= -\frac{1}{i\kappa_0 \eta_0} \mathbf{curl} \mathbf{e}^{inc}(\mathbf{x}), \end{aligned}$$

where $\hat{\mathbf{x}}$ and $\hat{\mathbf{z}}$ denote the unit vectors along the x -axis and z -axis, respectively.

Fig. 3 displays the magnitude of the electric current density $\mathbf{n} \times \mathbf{h}$ on the boundaries of the three domains, computed using the mixed MT-Müller formulation (11). In all cases, the structures are excited by a plane wave with wavenumber $\kappa_0 = 6 \text{ m}^{-1}$. The computed currents exhibit the expected continuity across interfaces between adjacent materials.

A. Far-Field Evaluations

To assess the accuracy of secondary quantities produced by the proposed method, we evaluate the far-field patterns obtained from the surface current densities computed on the two-component sphere and compare them with the analytical Mie-series solutions [37]. Fig. 4 illustrates the scattered electric far fields for two incident plane waves with wavenumbers $\kappa_0 = 6 \text{ m}^{-1}$ and $\kappa_0 = 0.06 \text{ m}^{-1}$. In both cases, the MT-Müller

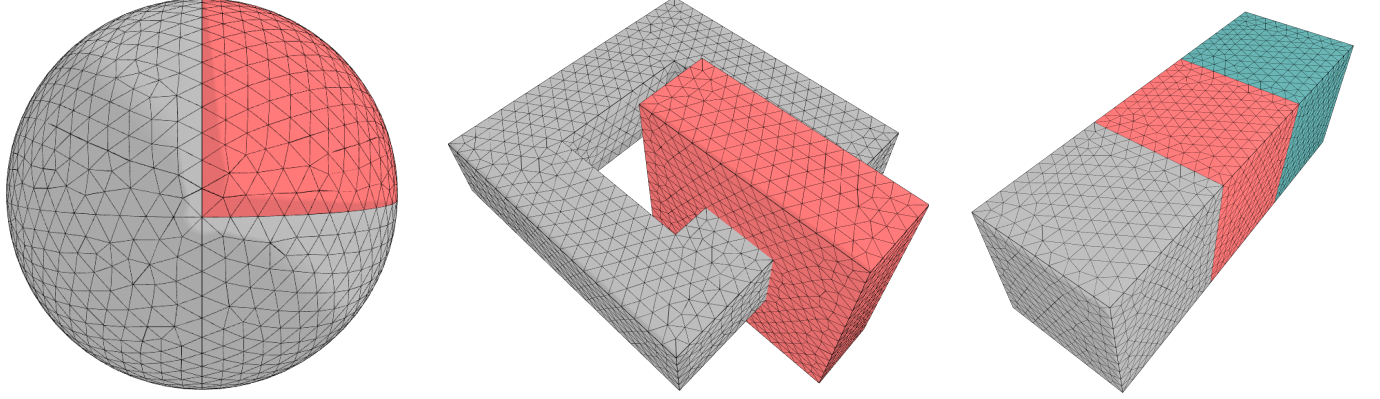


Fig. 2. Geometries used in numerical experiments. From left to right: a two-component unit sphere in which one component occupies three quadrants and the other occupies the remaining quadrant; a configuration of two fused square-section tori featuring a fully occluded cavity; and a domain constructed by stacking multiple unit cubes (illustrated here using three cubes).

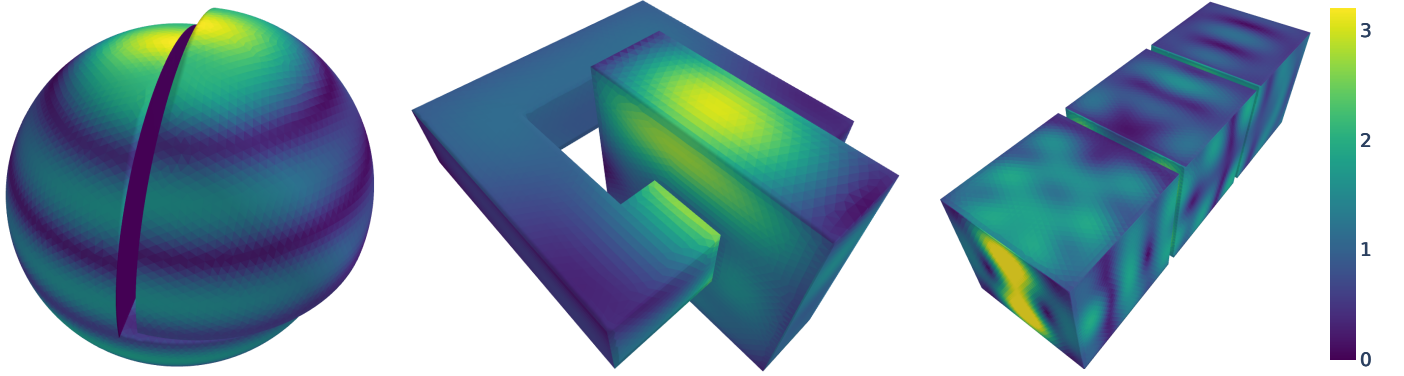


Fig. 3. Magnitude of the electric surface current density on the boundaries of the three geometries, excited by a plane wave with wavenumber $\kappa_0 = 6 \text{ m}^{-1}$, computed using the global multi-trace Müller equation. For visualization purposes, the subdomains of the sphere (leftmost) and the cubes (rightmost) are slightly separated. The solutions exhibit continuity across the interfaces between adjacent materials.

formulation reproduces the exact far fields with high fidelity, demonstrating that the mixed discretization remains accurate across moderate and high-frequency regimes.

In the low-frequency limit, the solenoidal and irrotational components of the trace solution may scale differently, leading to numerical cancellation when both components are stored within a single floating-point variable. This cancellation results in inaccurate far-field computations [38], [39]. As shown in [21], the mixed Müller formulation produces traces with the correct scaling up to frequencies that solely depend on quadrature and machine precisions, thereby allowing for the introduction of a stabilization scheme. However, a detailed investigation of low-frequency stabilization techniques for the Müller and MT-Müller formulations lies beyond the scope of the present work and will be addressed in a forthcoming study.

B. Extinction Property

Next, we validate the correctness of the proposed MT-Müller formulation by examining the extinction property (1) and the continuity of the derived near fields for the simulation shown in Fig. 3 (middle). The electric and magnetic fields are reconstructed both inside and outside the dual-torus structure using the Stratton-Chu representation potentials. Fig. 5

presents the reconstructed electric field evaluated on a grid at $y = 0.5\text{m}$. The first three subplots correspond to the fields generated using the potentials associated with the material coefficients of the background region and the two interior subdomains, while the final subplot shows the total electric field obtained by summing the contributions from all regions.

The reconstructed fields confirm that the computed surface currents satisfy the extinction property, therefore constitute a solution to Maxwell's equations. Moreover, the total field exhibits the continuity across material interfaces. These observations demonstrate that the proposed MT-Müller formulation correctly enforces transmission conditions within the discretization error and provides an accurate boundary representation of the scattering problem.

C. Conditioning

The defining advantage of second-kind BIEs over their first-kind counterparts lies in their favorable conditioning properties. To substantiate this advantage for the proposed MT-Müller formulation, we investigate its numerical conditioning by examining both the condition number of the resulting system matrix \mathbb{M} and the number of GMRES iterations required to

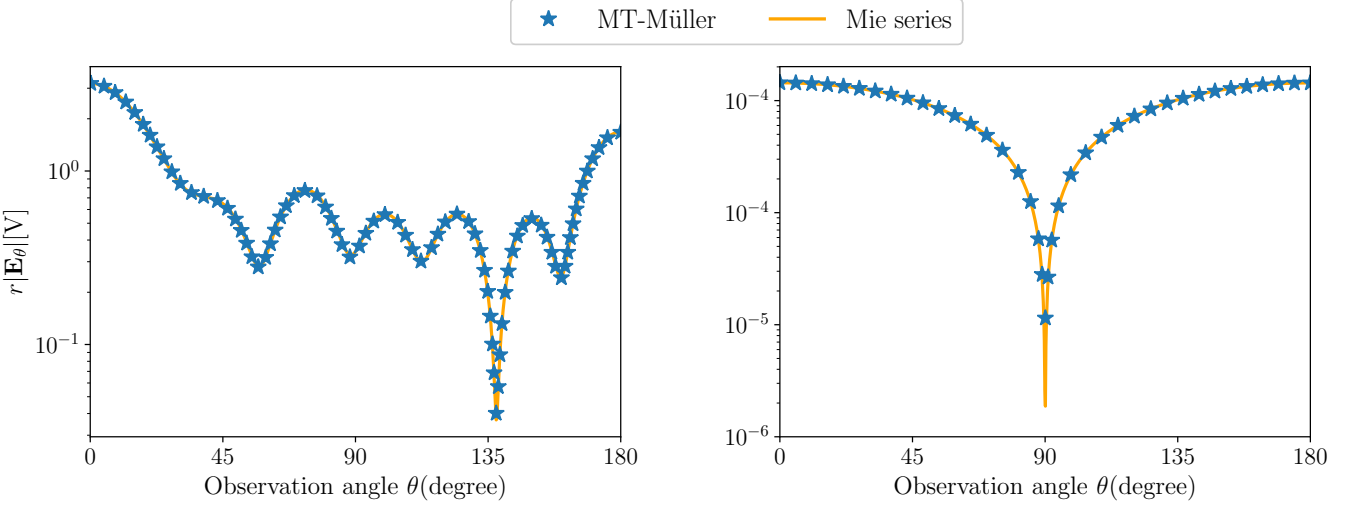


Fig. 4. Electric far field scattered by the unit sphere for incident plane waves with wavenumbers $\kappa_0 = 6 \text{ m}^{-1}$ (left) and $\kappa_0 = 0.06 \text{ m}^{-1}$ (right). The far fields computed using the MT-Müller formulation show excellent agreement with those obtained from the Mie series.

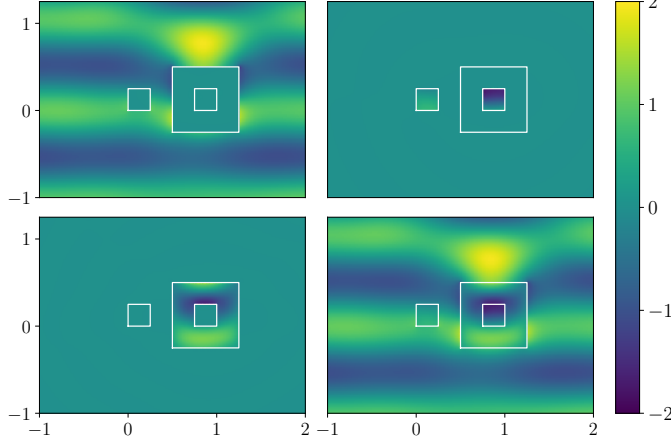


Fig. 5. Real part of the y -component of the electric field reconstructed from the Cauchy data on the interfaces of the dual-torus domain using the Stratton-Chu representation potentials, evaluated on a grid at $y = 0.5\text{m}$. From top to bottom and left to right, the subplots show the fields reconstructed using the potentials associated with the background region, with the two subdomains, and finally the total electric field. The surface currents fulfill the extinction property and therefore constitute a Maxwell solution. The total field also exhibits the continuity across the material interfaces.

reach a prescribed convergence tolerance, over a broad range of mesh resolutions and frequencies.

The dual-torus domain is chosen as a particularly revealing test geometry due to its non-trivial topological structure. Each subdomain is itself a torus with genus $g = 1$, while the boundary of the complement region Ω_0 is also multiply connected with genus $g = 1$ (as a consequence of the occlusion of an interior cavity), leading to a strongly coupled topology. It is well known that the static interior and exterior magnetic field integral operators $\frac{1}{2}I \pm \tilde{K}$, with \tilde{K} denoting the zero-frequency double-layer BIO, possess non-trivial nullspaces on toroidal surfaces. As the frequency tends to zero, these nullspaces manifest numerically as a growth in the condition number of the corresponding discretized operators [40]. The

intricate topology of the dual-torus geometry suggests that the proposed MT-Müller operator may exhibit a similar growth in its condition number when the frequency approaches zero, since all of its blocks involve either the weighted summation or subtraction of two magnetic field integral operators on their diagonals.

For comparison, we recall the standard discretization of the MT-PMCHWT equation (5)

$$\mathbb{P}\mathbf{u} = \hat{\mathbf{u}}^{inc}, \quad (12)$$

where \mathbb{P} is the matrix representation of the bilinear form $\langle \cdot, P \cdot \rangle_{\times}$ on $\mathbb{RT}(\Gamma_h) \times \mathbb{RT}(\Gamma_h)$ and $\hat{\mathbf{u}}^{inc}$ is the vector corresponding to the linear functional $\langle \cdot, \mathbf{u}^{inc} \rangle_{\times}$ on $\mathbb{RT}(\Gamma_h)$.

Fig. 6 presents the condition numbers and GMRES iteration counts for the mixed MT-Müller discretization (11) and the MT-PMCHWT formulation (12) as functions of the wavenumber κ_0 and the mesh size h . The results clearly demonstrate that the MT-Müller equation remains well-conditioned as κ_0 and h tend to zero. In contrast, the MT-PMCHWT formulation exhibits rapidly increasing condition numbers and iteration counts under mesh refinement and in the low-frequency regime. The non-increasing condition number at extremely low frequencies further indicates that the proposed MT-Müller formulation does not admit any non-trivial nullspaces, even on toroidal surfaces and in topologically complex geometries such as the dual-torus domain.

D. Computational Time

In the final experiment, we investigate the computational performance of the mixed MT-Müller formulation (11) in comparison with the standard MT-PMCHWT formulation (12) and its CP variants. Specifically, we consider the following CP MT-PMCHWT formulation [10]:

$$\mathbb{T}\mathbb{G}^{-1}\mathbb{P}\mathbf{u} = \mathbb{T}\mathbb{G}^{-1}\hat{\mathbf{u}}^{inc}, \quad (13)$$

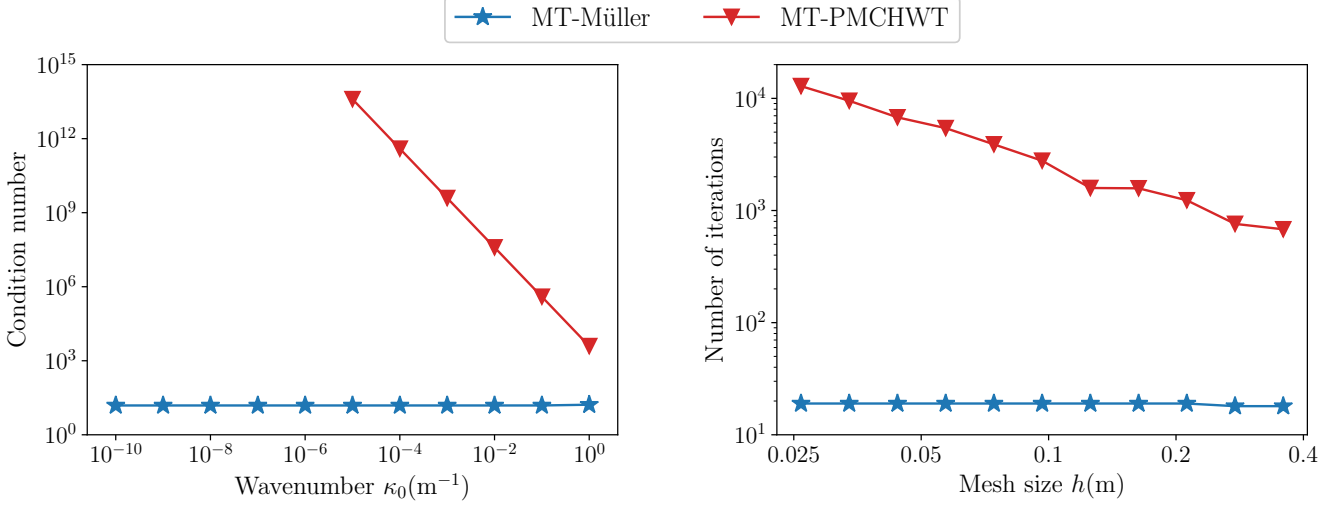


Fig. 6. Conditioning behavior of the MT-Müller and MT-PMCHWT formulations. *Left*: Condition number as a function of the wavenumber κ_0 , with the mesh size fixed at $h = 0.1$ m. *Right*: Number of GMRES iterations required to reach a relative tolerance of 10^{-6} as a function of the mesh size h , with $\kappa_0 = 1$ m⁻¹. The condition number and GMRES iteration count of the MT-Müller equation remain constant as κ_0 and h tend to zero. In contrast, the MT-PMCHWT formulation exhibits rapidly deteriorating conditioning, with both metrics increasing significantly under mesh refinement and at low frequencies.

where \mathbb{T} and \mathbb{G} are block-diagonal matrices whose diagonal entries are given by

$$[\mathbb{T}]_{kk} = \begin{pmatrix} \mathbf{0} & \mathbb{T}_k \\ -\mathbb{T}_k & \mathbf{0} \end{pmatrix}, \quad [\mathbb{G}]_{kk} = \begin{pmatrix} \mathbb{G}_k & \mathbf{0} \\ \mathbf{0} & \mathbb{G}_k \end{pmatrix},$$

for $k = 1, 2, \dots, N$. Here, the local Gram matrix \mathbb{G}_k represents the bilinear form $\langle \cdot, I \cdot \rangle_{\times, k}$ on $\text{RT}(\Gamma_{h,k}) \times \text{BC}(\Gamma_{h,k})$, while \mathbb{T}_k is the matrix representation of $\langle \cdot, \tilde{T}_{kk} \cdot \rangle_{\times, k}$ on $\text{BC}(\Gamma_{h,k}) \times \text{BC}(\Gamma_{h,k})$. The Yukawa-type single-layer operators \tilde{T}_{kk} are obtained from the operators $T_{kk}^{(0)}$ by replacing the wavenumber κ_0 with the purely imaginary value $-\iota\kappa_0$ [41].

Fig. 7 summarizes the measured assembly and solving times for the three formulations as the number of components N increases. The MT-PMCHWT formulation exhibits minimal assembly costs but suffers from prohibitively large solution times, making preconditioning crucial. The CP MT-PMCHWT formulation (13) significantly reduces the solution time at the expense of additional assembly work associated with the construction of the Calderón preconditioner, resulting in a substantially improved overall performance. This overhead is already mitigated by employing a diagonal Calderón preconditioner and would increase further if a full Calderón preconditioner were used instead.

In contrast, the mixed MT-Müller formulation (11) incurs higher assembly costs due to barycentric mesh refinement and the increased number of BIOs, but consistently achieves the shortest solution times. As a result, its total runtime is comparable to that of the CP MT-PMCHWT formulation. The short solving times are particularly advantageous in applications involving multiple right-hand sides. Moreover, in low-frequency regimes where the MT-PMCHWT formulations experience deteriorating conditioning, the mixed MT-Müller formulation remains robust.

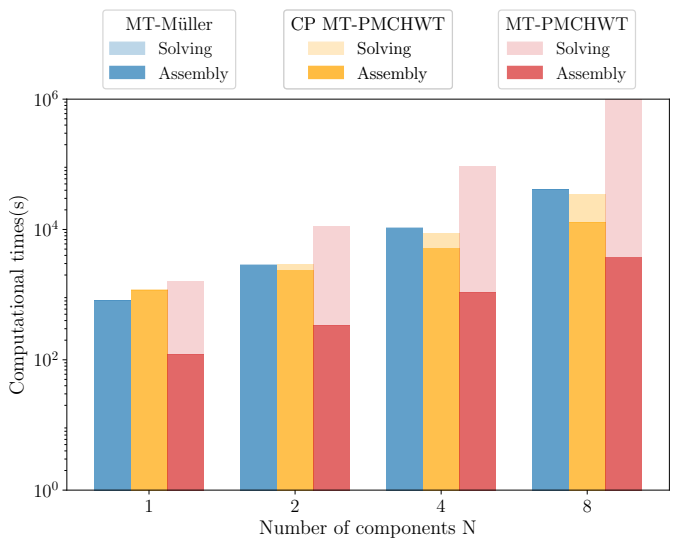


Fig. 7. Assembly and solving times for different boundary integral formulations applied to electromagnetic scattering by a vertical stack of unit cubes, shown as a function of the number of cubes N . A single plane-wave excitation with background wavenumber $\kappa_0 = 0.01$ m⁻¹ is considered. A uniform triangulation with mesh size $h = 0.07$ m yields $N_{e,k} = 4890$ edges (corresponding to 9780 unknowns) per cube. The solving times for the mixed MT-Müller formulation fall below the resolution of the plot.

V. CONCLUSION

We have introduced a global multi-trace Müller boundary integral formulation for electromagnetic scattering by composite dielectric objects, composed exclusively of second-kind operators. Employing a conforming mixed discretization based on RWG and BC basis functions, the method delivers accurate trace solutions and derived electromagnetic quantities while exhibiting favorable conditioning on dense meshes and in low-frequency regimes. From a computational perspective, the mixed MT-Müller formulation achieves significantly reduced solution times. Although it entails increased assembly costs,

its overall computational time remains comparable to that of Calderón-preconditioned PMCHWT formulations in typical configurations. In scenarios involving multiple excitations, where solution efficiency dominates the total runtime, the MT-Müller formulation offers a particularly compelling advantage, establishing it as a highly competitive alternative for large-scale and repeated-scattering simulations.

As already mentioned in the introduction, an important direction for future research concerns the extension of the proposed formulation to time-domain problems. Future work will therefore focus on a systematic investigation of TD-Müller formulations and on extending the multi-trace framework to transient electromagnetic scattering.

REFERENCES

- [1] Y. P. Chen, J. Jiang, S. Sun, W. C. Chew, and J. Hu, “Calderón preconditioned PMCHWT equations for analyzing penetrable objects in layered medium,” *IEEE Trans. Antennas Propag.*, vol. 62, no. 11, pp. 5619–5627, 2014.
- [2] A. Kleanthous, T. Betcke, D. P. Hewett, M. W. Scroggs, and A. J. Baran, “Calderón preconditioning of pmchwt boundary integral equations for scattering by multiple absorbing dielectric particles,” *J. Quant. Spectrosc. Radiat. Transfer*, vol. 224, pp. 383–395, 2019.
- [3] K. Cools, “Fast converging single trace quasi-local pmchwt equation for the modelling of composite systems,” *preprint*, 2025.
- [4] Z. Peng, K.-H. Lim, and J.-F. Lee, “Computations of electromagnetic wave scattering from penetrable composite targets using a surface integral equation method with multiple traces,” *IEEE Trans. Antennas Propag.*, vol. 61, no. 1, pp. 256–270, 2013.
- [5] Z. Peng, “A novel multitrace boundary integral equation formulation for electromagnetic cavity scattering problems,” *IEEE Trans. Antennas Propag.*, vol. 63, no. 10, pp. 4446–4457, 2015.
- [6] R. Zhao, Z. Huang, W.-F. Huang, J. Hu, and X. Wu, “Multiple-traces surface integral equations for electromagnetic scattering from complex microstrip structures,” *IEEE Trans. Antennas Propag.*, vol. 66, no. 7, pp. 3804–3809, 2018.
- [7] Y. Chu, W. C. Chew, J. Zhao, and S. Chen, “A surface integral equation formulation for low-frequency scattering from a composite object,” *IEEE Trans. Antennas Propag.*, vol. 51, no. 10, pp. 2837–2844, 2003.
- [8] P. Yla-Oijala, S. P. Kiminki, and S. Jarvenpaa, “Calderon preconditioned surface integral equations for composite objects with junctions,” *IEEE Trans. Antennas Propag.*, vol. 59, no. 2, pp. 546–554, 2011.
- [9] X. Claeys and R. Hiptmair, “Electromagnetic scattering at composite objects : a novel multi-trace boundary integral formulation,” *ESAIM Math. Model. Numer. Anal.*, vol. 46, no. 6, pp. 1421–1445, 2012.
- [10] S. Lasisi, T. M. Benson, G. Gradoni, M. Greenaway, and K. Cools, “A fast converging resonance-free global multi-trace method for scattering by partially coated composite structures,” *IEEE Trans. Antennas Propag.*, vol. 70, no. 10, pp. 9534–9543, 2022.
- [11] C. Müller, *Foundations of the mathematical theory of electromagnetic waves*. Springer Berlin Heidelberg, 1969.
- [12] Y. Zhang, T. J. Cui, W. C. Chew, and J.-S. Zhao, “Magnetic field integral equation at very low frequencies,” *IEEE Trans. Antennas Propag.*, vol. 51, no. 8, pp. 1864–1871, 2003.
- [13] P. Ylä-Oijala, M. Taskinen, and S. Järvenpää, “Analysis of surface integral equations in electromagnetic scattering and radiation problems,” *Eng. Anal. Bound. Elem.*, vol. 32, no. 3, pp. 196–209, 2008.
- [14] J. Kornprobst and T. F. Eibert, “Accuracy analysis of div-conforming hierarchical higher-order discretization schemes for the magnetic field integral equation,” *IEEE J. Multiscale Multiphysics Comput. Tech.*, vol. 8, pp. 261–268, 2023.
- [15] A. Buffa and S. H. Christiansen, “A dual finite element complex on the barycentric refinement,” *Math. Comp.*, vol. 76, no. 260, pp. 1743–1770, 2007.
- [16] Q. Chen and D. R. Wilton, “Electromagnetic scattering by three-dimensional arbitrary complex material/conducting bodies,” in *Proc. Int. Symp. Antennas Propag. Soc., Merging Technol.*, vol. 2, 1990, pp. 590–593.
- [17] M. S. Tong, W. C. Chew, B. J. Rubin, J. D. Morsey, and L. Jiang, “On the dual basis for solving electromagnetic surface integral equations,” *IEEE Trans. Antennas Propag.*, vol. 57, no. 10, pp. 3136–3146, 2009.
- [18] K. Cools, F. P. Andriulli, D. De Zutter, and E. Michielssen, “Accurate and conforming mixed discretization of the MFIE,” *IEEE Antennas Wirel. Propag. Lett.*, vol. 10, pp. 528–531, 2011.
- [19] H. A. Ülkü, I. Bogaert, K. Cools, F. P. Andriulli, and H. Bağci, “Mixed discretization of the time-domain MFIE at low frequencies,” *IEEE Antennas Wirel. Propag. Lett.*, vol. 16, pp. 1565–1568, 2017.
- [20] S. Yan, J.-M. Jin, and Z. Nie, “Accuracy improvement of the second-kind integral equations for generally shaped objects,” *IEEE Trans. Antennas Propag.*, vol. 61, no. 2, pp. 788–797, 2013.
- [21] I. Bogaert, K. Cools, F. P. Andriulli, and H. Bagci, “Low-frequency scaling of the standard and mixed magnetic field and Müller integral equations,” *IEEE Trans. Antennas Propag.*, vol. 62, no. 2, pp. 822–831, 2014.
- [22] V. C. Le and K. Cools, “Boundary element methods for the magnetic field integral equation on polyhedra,” *preprint*, 2024.
- [23] M. Taskinen and P. Yla-Oijala, “Current and charge integral equation formulation,” *IEEE Trans. Antennas Propag.*, vol. 54, no. 1, pp. 58–67, 2006.
- [24] B. Shanker, M. Lu, J. Yuan, and E. Michielssen, “Time domain integral equation analysis of scattering from composite bodies via exact evaluation of radiation fields,” *IEEE Trans. Antennas Propag.*, vol. 57, no. 5, pp. 1506–1520, 2009.
- [25] X. Claeys, R. Hiptmair, and E. Spindler, “Second-kind boundary integral equations for electromagnetic scattering at composite objects,” *Comput. Math. Appl.*, vol. 74, no. 11, pp. 2650–2670, 2017.
- [26] V. C. Le, V. Giunzioni, P. Cordel, F. P. Andriulli, and K. Cools, “On the late-time instability of MOT solution to the time-domain PMCHWT equation,” *IEEE Antennas Wirel. Propag. Lett.*, vol. 24, no. 12, pp. 4720–4724, 2025.
- [27] V. C. Le, C. Münger, F. P. Andriulli, and K. Cools, “A stable, accurate and well-conditioned time-domain PMCHWT formulation,” *preprint*, 2025.
- [28] D. Colton and R. Kress, *Inverse acoustic and electromagnetic scattering theory*, 3rd ed., ser. Applied Mathematical Sciences. Springer, 2013, vol. 93.
- [29] S. Rao, D. Wilton, and A. Glisson, “Electromagnetic scattering by surfaces of arbitrary shape,” *IEEE Trans. Antennas Propag.*, vol. AP-30, no. 3, pp. 409–418, 1982.
- [30] S. B. Adrian, F. P. Andriulli, and T. F. Eibert, “On a refinement-free Calderón multiplicative preconditioner for the electric field integral equation,” *J. Comput. Phys.*, vol. 376, pp. 1232–1252, 2019.
- [31] I. Fierro-Piccardo and T. Betcke, “An OSRC preconditioner for the EFIE,” *IEEE Trans. Antennas Propag.*, vol. 71, no. 4, pp. 3408–3417, 2023.
- [32] M. Bebendorf, “Approximation of boundary element matrices,” *Numer. Math.*, vol. 86, no. 4, pp. 565–589, 2000.
- [33] J. M. Tetzner and S. B. Adrian, “On the adaptive cross approximation for the magnetic field integral equation,” *IEEE Trans. Antennas Propag.*, vol. 72, no. 12, pp. 9366–9377, 2024.
- [34] S. Börm, L. Grasedyck, and W. Hackbusch, “Introduction to hierarchical matrices with applications,” *Eng. Anal. Bound. Elem.*, vol. 27, no. 5, pp. 405–422, 2003.
- [35] V. Rokhlin, “Rapid solution of integral equations of scattering theory in two dimensions,” *J. Comput. Phys.*, vol. 86, no. 2, pp. 414–439, 1990.
- [36] R. Coifman, V. Rokhlin, and S. Wandzura, “The fast multipole method for the wave equation: a pedestrian prescription,” *IEEE Antennas Propag. Mag.*, vol. 35, no. 3, pp. 7–12, 1993.
- [37] B. Hofmann, P. Respondek, and S. B. Adrian, “SphericalScattering: A Julia package for electromagnetic scattering from spherical objects,” *J. Open Source Softw.*, vol. 8, no. 91, p. 5820, 2023.
- [38] S. B. Adrian, A. Dely, D. Consoli, A. Merlini, and F. P. Andriulli, “Electromagnetic integral equations: insights in conditioning and preconditioning,” *IEEE Open J. Antennas Propag.*, vol. 2, pp. 1143–1174, 2021.
- [39] V. C. Le, P. Cordel, F. P. Andriulli, and K. Cools, “A stabilized time-domain combined field integral equation using the quasi-Helmholtz projectors,” *IEEE Trans. Antennas Propag.*, vol. 72, no. 7, pp. 5852–5864, 2024.
- [40] K. Cools, F. P. Andriulli, F. Olyslager, and E. Michielssen, “Nullspaces of MFIE and Calderón preconditioned EFIE operators applied to toroidal surfaces,” *IEEE Trans. Antennas Propag.*, vol. 57, no. 10, pp. 3205–3215, 2009.
- [41] V. C. Le and K. Cools, “An operator preconditioned combined field integral equation for electromagnetic scattering,” *SIAM J. Numer. Anal.*, vol. 62, no. 6, pp. 2484–2505, 2024.